# The Use of Rosseland- and Planck-Averaged Opacities in Multigroup Radiation Diffusion

Pranav Devarakonda

*Brighton High School, 1150 Winton Road, Rochester, NY*

*LLE Advisor: Dr. Reuben Epstein*

*Laboratory for Laser Energetics, University of Rochester, Rochester, NY*

*August 2015*

**Abstract**

Opacity quantifies how strongly radiation is absorbed while passing through a material. Hydrocodes at LLE and elsewhere use opacity values averaged over large intervals of the radiation spectrum to calculate radiation energy diffusion transport within plasmas. This work compares two-opacity modeling, where Planck averages are used for emission and absorption and Rosseland averages are used for transport, with the treatment in LLE hydrocodes where a single opacity (typically the Planck average) is used. Planck and Rosseland interval-averaged opacities for Si were obtained by running the Prism detailed atomic model *PROPACEOS*. An analytic solution was then derived for the radiation diffusion equation in a slab-source problem in which separate opacities were used for absorption and transport. Results for the emitted spectral flux were compared for the preferred two-opacity case and for the case where a single, Planck opacity was used. Even when the Planck and Rosseland averages differed, the differences in flux were minimal except for spectral intervals where the optical depth was approximately 1.

# 1. Introduction

At the University of Rochester's Laboratory for Laser Energetics (LLE) and the National Ignition Facility (NIF),[1] research is done on laser fusion where laser energy is used to compress a capsule, bringing its fuel contents to thermonuclear fusion conditions.[2] There are two main types of laser fusion: direct drive and indirect drive. The Laboratory for Laser Energetics deals mainly with direct drive. In direct drive, a capsule's outer surface is irradiated directly by the laser beams, as opposed to indirect drive, where the inner surface of a small container enclosing the capsule is irradiated by laser beams entering the enclosure through laser entrance holes, generating thermal radiation that implodes the capsule.

The target is a spherical cryogenic capsule approximately 10 μm thick with a diameter of ~860 μm, coated on the inside with approximately 65 μm of deuterium-tritium (DT) ice, and filled with three atmospheres of DT. [3] The laser is the 60 beam OMEGA laser system, [4] one of the most powerful in the world. During direct-drive inertial confinement fusion, the laser pulses partially ablate the surface of the capsule, causing it to rocket off, and compress the capsule, along with its DT contents, to conditions of high temperature and density. At a sufficiently high temperature, the deuterium and tritium undergo fusion reactions to form helium, a neutron, and large amounts of energy. A large amount of thermal energy is needed to give the colliding nuclei the large thermal velocities needed to overcome their large electrostatic repulsion.

The amount of energy produced by the inertial confinement fusion process can be inferred from the measured neutron yield. LLE uses simulation programs, such as the one-dimensional hydrodynamics code LILAC,[5] to predict the outcome of these experiments. A significant factor affecting the outcome of inertial confinement fusion experiments is the x-ray opacity of the imploding capsule. Opacity is a measure of impenetrability of electromagnetic or

other kinds of radiation.[6,7] The current hydrodynamic codes use one type of averaged spectral-interval opacity, the Planck-averaged opacity. This work explores whether Rosseland-averaged opacity should also be used in the computational codes.[8]

## 2. Equations of Radiative Transfer

The hydrodynamic simulation code LILAC[5] is one of several used at the Laboratory for Laser Energetics that includes a radiation diffusion transport model. The codes are all similar, in that they all compute several important quantities such as radiation energy density $U_\nu$, the spectral flux $F_\nu$, scale length $\lambda_\nu$, and optical depth $\tau_\nu$. These quantities are functions of the spectral frequency $\nu$ of the radiation and the local temperature $T$ and material density. LILAC is unique in that it models plasma flow with spherical, cylindrical, or planar symmetry and spatial variation in only one dimension. Consequently, in this work, where we consider how radiation transport might be done differently, 1D radiation transport, as LILAC does it, is a logical point of reference. Other simulation codes at LLE use radiative opacity in similar ways, so the lessons learned in this work will have relevance to them as well.

Opacity is defined as the quantitative measure of how strongly radiation is absorbed while passing through a material. Optical depth is a dimensionless quantity defined as the integral of opacity with respect to distance. If the optical depth is much greater than 1, the source is considered to be optically thick, and, conversely, if the optical depth of the source is much less than 1, the source is considered to be optically thin. The following equation expresses the optical depth at the spectral frequency $\nu$:

$$\tau_\nu = \int \kappa_\nu ds, \tag{2.1}$$

where $\kappa_\nu$ is the opacity at frequency $\nu$ and $s$ is the distance along a path through the source. The value of the optical depth depends on the choice of this path.[6,7] The quantities of spectral flux $F_\nu$ and radiation energy density $U_\nu$ are closely related in the time-independent diffusion approximation by the following equations,

$$F_\nu = -\frac{c}{3\kappa_\nu}\frac{dU_\nu}{ds} \tag{2.2a}$$

$$\frac{dF_\nu}{ds} = \varepsilon_\nu - c\kappa_\nu U_\nu, \tag{2.2b}$$

where $c$ is the speed of light and $\varepsilon_\nu$ is emissivity (emitted spectral power per unit volume) at frequency $\nu$.[8] Equations (2.2) are written for 1D plane-parallel geometry where the path length parameter $s$ is the spatial coordinate in the one spatial dimension. The diffusion approximation arises from the assumption that radiation is defined as a locally isotropic spectral energy density of photons plus a small flux in a single direction along the gradient of $U_\nu$. Equation (2.2a) gives the magnitude of this radiation flux in terms of this gradient of the radiation energy density, and Eq. (2.2b) equates the divergence of this radiation flux to the total radiation emission-minus-absorption at a given point. Equations (2.2a) and (2.2b) can be solved simultaneously for $U_\nu$ and $F_\nu$. These two equations can be combined into one by eliminating $F_\nu$, leaving the more familiar diffusion equation, a 2nd-order differential equation for $U_\nu$,[8]

$$0 = -\frac{d}{ds}\left(\frac{c}{3\kappa_\nu}\frac{dU_\nu}{ds}\right) + \varepsilon_\nu - c\kappa_\nu U_\nu. \tag{2.3}$$

When calculating radiation transport numerically over the whole spectrum, the spectrum is divided into a finite number of frequency intervals or "groups," where the spectral frequency group index $k$ refers to the frequency interval from $\nu_k$ to $\nu_{k+1}$. This frequency grouping should

be as fine as necessary to resolve the spectrum, but there should also be as few groups as possible to minimize the time and other computational resources required to complete the calculation. This "multigroup" formulation is constructed by replacing the frequency-dependent flux, energy density, emissivity, and opacity quantities in Eqs. 2.2a, 2.2b, and 2.3 with group-averaged quantities:

$$F_k = -\frac{c}{3\kappa_{R,k}}\frac{dU_k}{ds} \tag{2.4a}$$

$$\frac{dF_k}{ds} = \varepsilon_k - c\kappa_{P,k}U_k. \tag{2.4b}$$

The group-averaged emissivity is obtained using

$$\varepsilon_k = \frac{\int_{\upsilon_k}^{\upsilon_{k+1}} \varepsilon_\upsilon d\upsilon}{\upsilon_{k+1}-\upsilon_k}, \tag{2.5}$$

and the flux $F_k$ and energy density $U_k$ averages are obtained by the same method. [6,8]

For Eq. (2.4a) to be consistent with Eq. (2.2a), the group-average opacity $\kappa_{R,k}$ must be

$$\frac{1}{\kappa_{R,k}} = \frac{\int_{\nu_k}^{\nu_{k+1}} \frac{1}{\kappa_\nu}\frac{dU_\nu}{ds} d\nu}{\int_{\nu_k}^{\nu_{k+1}} \frac{dU_\nu}{ds} d\nu}, \tag{2.6a}$$

and for Eq. (2.4b) to be consistent with Eq. (2.2b), the group-average opacity $\kappa_{P,k}$ must be

$$\kappa_{P,k} = \frac{\int_{\nu_k}^{\nu_{k+1}} U_\nu \kappa_\nu d\nu}{\int_{\nu_k}^{\nu_{k+1}} U_\nu d\nu}. \tag{2.6b}$$

Equations (2.6) show that calculating the multigroup average opacity quantities requires that the radiation energy density $U_\nu$ frequency dependence be known in sub-group detail, i.e., in finer

spectral detail than the multigroup spectral resolution can provide. We can proceed with the multigroup method by approximating the weighting functions in Eqs. (2.6) with the radiation energy density known to exist under conditions of local thermodynamic equilibrium,[8]

$$U_\nu = \frac{4\pi}{c} B_\nu(T), \tag{2.7a}$$

where $B_\nu(T)$ is the Planck function

$$B_\nu(T) = \frac{2h\nu^3}{c^2} \frac{1}{e^{h\nu/k_B T} - 1}, \tag{2.8}$$

and where $h$ is the Planck constant and $k_B$ is the Boltzmann constant. This approximation was originally devised for the deep interior of stars, where it is an excellent approximation.[7] Other than this precedent, we have no well-developed justification for using this approximation in laser fusion. We can also write

$$\frac{dU_\nu}{ds} = \frac{4\pi}{c} \frac{dB_\nu(T)}{dT} \frac{dT}{ds}. \tag{2.7b}$$

The two kinds of opacity average which we will explore are the Planck-averaged opacity, obtained from Eqs. (2.6b) and (2.7a), computed as an arithmetic mean weighted by the Planck function,

$$\kappa_{P,k} \equiv \frac{\int_{\nu_k}^{\nu_{k+1}} B_\nu \kappa_\nu d\nu}{\int_{\nu_k}^{\nu_{k+1}} B_\nu d\nu}, \tag{2.9a}$$

and the Rosseland-averaged opacity, obtained from Eqs. (2.6a) and (2.7b), computed as a harmonic mean weighted by the derivative of the Planck function with respect to temperature,[8]

$$\frac{1}{\kappa_{R,k}} \equiv \frac{\int_{\nu_k}^{\nu_{k+1}} \frac{1}{\kappa_\nu} \frac{dB_\nu}{dT} d\nu}{\int_{\nu_k}^{\nu_{k+1}} \frac{dB_\nu}{dT} d\nu} \quad . \tag{2.9b}$$

The temperature gradient *dT/ds* in Eq. (2.7b) cancels out of the quotient in Eq. (2.6a).

Just as the arithmetic mean of a set of data is always greater than or equal to the harmonic mean, the Planck-averaged opacity is generally greater than or equal to the Rosseland-averaged opacity, assuming that the weighting functions do not greatly impact the averages. As the number of groups increases and as the individual groups narrow to the point where the spectral features of the opacity begin to be resolved by the frequency groups, the differences between the Planck and Rosseland averages become less important, and the choice of the weighting functions becomes less critical. Unfortunately, computational limits on spectral resolution may not allow a number of frequency groups large enough to achieve this.

The tabulated group-averaged emissivity $\varepsilon_k$ is generally obtained as part of the same atomic-physics calculation used to obtain the group-averaged opacity or opacities. Under conditions of local thermodynamic equilibrium, which is assumed here, the emissivity is related to the opacity by the Kirchoff relationship[9]

$$\varepsilon_\nu = 4\pi\kappa_\nu B_\nu(T). \tag{2.10}$$

Equation (2.7a) is, in part, a consequence of Eq. (2.10). Using Eq. (2.10) in Eq. (2.5) and applying Eq. (2.9a) gives the expression

$$\varepsilon_k = \frac{4\pi\kappa_{P,k} \int_{\nu_k}^{\nu_{k+1}} B_\nu(T) d\nu}{\nu_{k+1} - \nu_k}, \tag{2.11}$$

which relates the group-averaged emissivity $\mathcal{E}_k$ to the Planck-averaged opacity $\kappa_{P,k}$.

Consequently, $\mathcal{E}_k$ will not be changed by varying $\kappa_{R,k}$, as long as $\kappa_{P,k}$ is left constant.

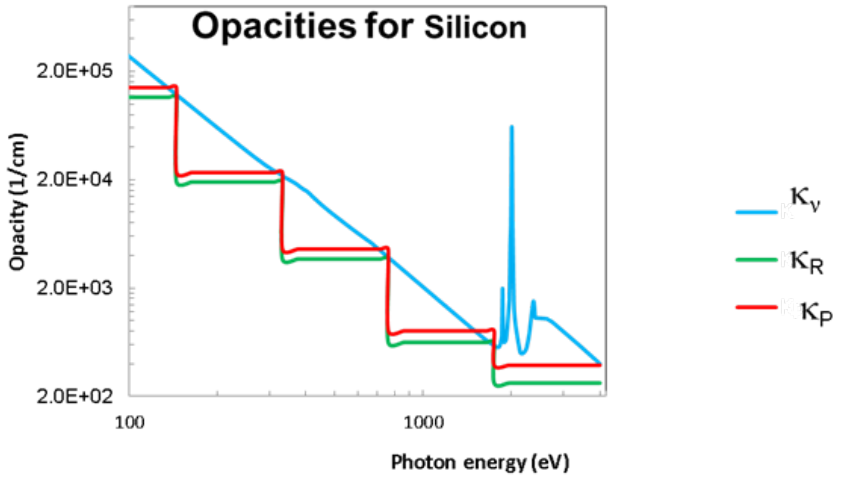


Fig. 1: A graph of the opacity ($\kappa_\nu$) of silicon and the Planck ($\kappa_P$) and Rosseland ($\kappa_R$) group-averaged opacities as functions of photon energy, for a density $n_i$ of $1.68 \times 10^{23}$ ions/cm$^3$ and a temperature of 1.93 keV.

Figure 1 shows the opacity $\kappa_\nu$ of silicon,[10] which is a possible target material, for typical laser-fusion values of ion density and temperature. The Planck and Rosseland-averaged opacities are in the form of step functions in Fig. 1 where the horizontal segments represent the opacity averaged over a photon energy interval. Photon energy and frequency are essentially equivalent terms, related through the Planck equation $E = h\nu$. In the regions where the opacity varies smoothly, the Planck and Rosseland-averaged opacities are roughly equal. However, when there is a spectral line, as is seen in the highest energy group at the right end of the ordinate where the opacity value spikes markedly, the Planck-averaged opacity is significantly larger than the Rosseland-averaged opacity.

In this work, two-opacity modeling, where the Planck average is used for emission (through Eq. (2.11)) and absorption in Eq. (2.4b) and the Rosseland average is used for transport in Eq. (2.4a), is compared with the single-opacity treatment in LLE hydrocodes where a single opacity (typically the Planck average) is used for all purposes.

## 3. The Slab Source Problem

The slab source problem is a common illustrative example in radiation transport literature. The slab source problem assumes a uniform slab of thickness $L$ under conditions of uniform composition, temperature, and density. This provides a slab with spatially uniform opacity and emissivity where the general solution to Eqs. (2.4a) and (2.4b) is

$$U_k(x) = C_0 - C_1 e^{\sqrt{3\kappa_{P,k}\kappa_{R,k}}x} - C_2 e^{-\sqrt{3\kappa_{P,k}\kappa_{R,k}}x}, \tag{3.1a}$$

and, by Eq. (2.4a),

$$F_k(x) = c\sqrt{\frac{\kappa_{P,k}}{3\kappa_{R,k}}}\left(C_1 e^{\sqrt{3\kappa_{P,k}\kappa_{R,k}}x} - C_2 e^{-\sqrt{3\kappa_{P,k}\kappa_{R,k}}x}\right), \tag{3.1b}$$

where $x$ is the spatial coordinate in the direction normal to the slab. The constant $C_0$ is determined by substitution into Eqs (2.4a) and (2.4b),

$$C_0 = \frac{\varepsilon_k}{c\kappa_{P,k}}, \tag{3.1c}$$

and the constants $C_1$ and $C_2$ are set by a zero-flux condition at the center plane of the slab and by a surface flux boundary condition. At the center plane of the slab, $x=0$, there is no net flux in either direction because the positive and negative $x$ directions are equivalent, so $C_1 = C_2$ from Eq. (3.1b). At the outer surfaces of the slab, $x = \pm L/2$ , the only flux is that of the radiation energy density at the surface escaping freely at the speed of light along all possible directions, distributed uniformly into the outgoing hemisphere of directions. This is expressed as

$$F_k\left(\pm\frac{L}{2}\right) = \pm\frac{c}{2}U_k\left(\pm\frac{L}{2}\right), \tag{3.1d}$$

which, using Eqs. (3.1a), (3.1b), and (3.1c), completes the solution with

$$C_1 = C_2 = C_0\frac{1}{\left(\frac{2}{\sqrt{3}}\sqrt{\frac{\kappa_{P,k}}{\kappa_{R,k}}}+1\right)e^{\sqrt{3\kappa_{P,k}\kappa_{R,k}}\frac{L}{2}}-\left(\frac{2}{\sqrt{3}}\sqrt{\frac{\kappa_{P,k}}{\kappa_{R,k}}}-1\right)e^{-\sqrt{3\kappa_{P,k}\kappa_{R,k}}\frac{L}{2}}}. \tag{3.1e}$$

Examination of Eqs. (3.1a) and (3.1b) reveals that the spatial dependence of the flux and energy density in one photon energy group is entirely exponential of the form $e^{\pm x/\lambda_{PR,k}}$ with a single scale length $\lambda_{PR,k}$ where

$$\lambda_{PR,k} \equiv 1/\sqrt{3\kappa_{P,k}\kappa_{R,k}}, \tag{3.2}$$

and an optical thickness

$$\tau_{PR,k} \equiv L/\lambda_{PR,k}. \tag{3.3}$$

For sources that are optically thick, Eq. (3.1e) shows that the coefficients $C_1$ and $C_2$ vanish exponentially, relative to $C_0$, for large $\tau_{PR,k}$. This means that $U_k$ is very nearly equal to $C_0$ everywhere, except within a distance less than about one scale length inside of each of the outer surfaces of the slab. This is consistent with the interpretation that the energy density deep (optically) within a slab is determined almost completely by the balance of absorption and emission, leaving a flat energy density profile and, locally, a negligible flux, according to Eq. (2.4a), and, therefore, a negligible divergence of flux on the left-hand side of Eq. (2.4b) to modify the balance of absorption and emission expressed by the right-hand side of this equation.

By applying Eqs. (3.1) to the slab source problem, we can determine the spectral flux and energy density at various points in the source, most importantly at the outer surfaces. The material that we have chosen to explore as part of the slab source problem is silicon. This is

because other elements commonly used in laser fusion capsule shells such as hydrogen and carbon do not have spectral lines at typical temperatures because their electrons have already been freed and no longer undergo frequent transitions between discrete bound states. The sample temperature and ionic density which we have chosen to use is a temperature of 1.93 keV and an ionic density of $2.67 \times 10^{23}$ ions/cm$^3$ as these values correspond to typical conditions in which the silicon spectrum contains interesting features, including some spectral lines. [10]

The majority of the simulation codes at the Laboratory for Laser Energetics do not simultaneously use both the Rosseland-averaged and Planck-averaged opacities, a relic from the days of limited storage and processing capacity. One simulation code, Helios, by Prism Computational Sciences, Inc.,[11] uses both Planck-averaged and Rosseland-averaged opacities in its multigroup radiation transport model. The modeling of the radiation diffusion equations typically uses the Planck-averaged opacity in place of the Rosseland-averaged opacity for flux. The effect of the resulting inaccuracy on the results of radiation simulation can be assessed by repeating the simulation with successively finer frequency groupings until the results are no longer changed by further refinement. This process will eventually converge, since the Rosseland and Planck averages are equal in the limit of fine spectral resolution.

To demonstrate the impact of using a single-opacity (or one-opacity) Planck-averaged opacity instead of the more correct two-opacity model on the calculated radiation energy density and spectral flux, we explored two cases of a single energy group with Planck optical thicknesses $\tau_{P,k} = 3$ and 1, where

$$\tau_{P,k} \equiv L/\lambda_{P,k}, \tag{3.4}$$

expressed in terms of a Planck scale length

$$\lambda_{P,k} \equiv 1/\left(\sqrt{3}\kappa_{P,k}\right), \tag{3.5}$$

to illustrate what happens when the slab is of moderate optical thickness. Results are shown in Fig. 2 for various ratios of the Rosseland-averaged opacity to the Planck-averaged opacity. In these figures, $x$ represents the position across the thickness of the slab, plotted as the dimensionless quantity $x/L$, energy density is plotted in units of $C_0$, and flux is plotted in units of $cC_0$.

Figure 2(a) shows energy density profiles, and Fig. 2(b) shows radiation flux profiles of a slab of Planck optical thickness 3 for different values of the Rosseland-to-Planck opacity ratio. It is seen that there is little change in either graph when the Rosseland-averaged opacity is reduced to only half of the Planck-averaged opacity. Figure 2(c) shows the corresponding energy density profiles, and Fig. 2(d) shows the corresponding radiation flux profiles of a slab of Planck optical thickness 1. It is seen that by having reduced the optical thickness from 3 to 1, significantly less energy is bottled up in the slab, and the changes in the energy density and radiation flux with the reduction in the Rosseland opacity are still small. The more optically thin slab confines the escaping radiation less than in the more optically thick case, so the flux in Fig. 2(d) is more uniformly diverging and less affected by the Rosseland opacity value than in Fig. 2(b). In the examples studied thus far, no stronger or more dramatic effects than these of varying the Rosseland-to-Planck average opacity ratio have been found.

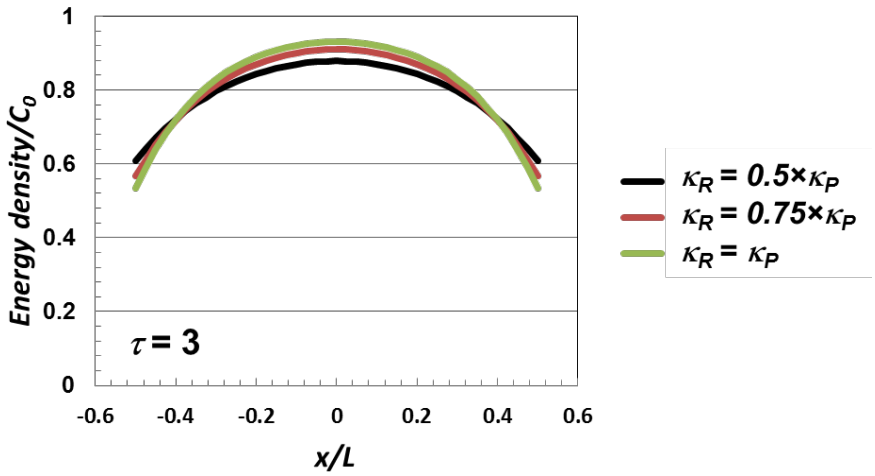


Fig. 2a: Energy density, in units of $C_0$, plotted as a function of position across the slab in units of the slab thickness $L$, within a slab of Planck optical thickness 3, for various ratios of $\kappa_R/\kappa_P$.

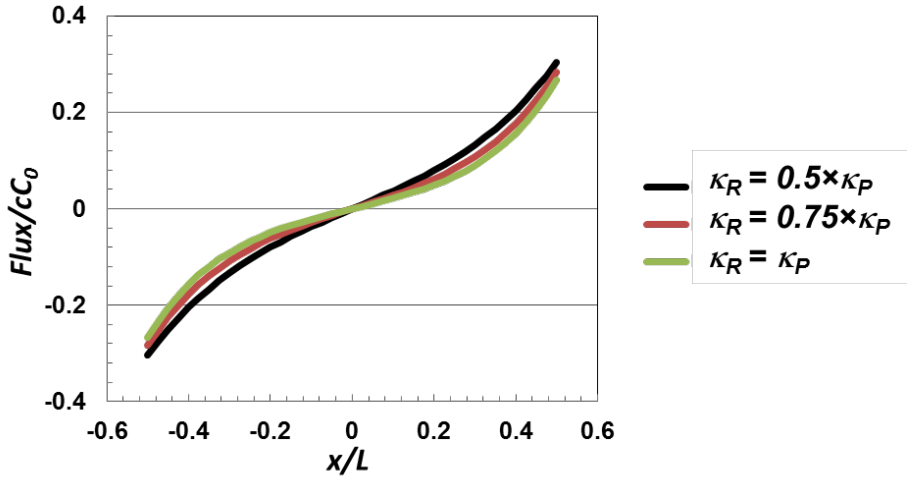


Fig. 2b: As Fig. 2a, but for spectral flux, plotted in units of $cC_0$.

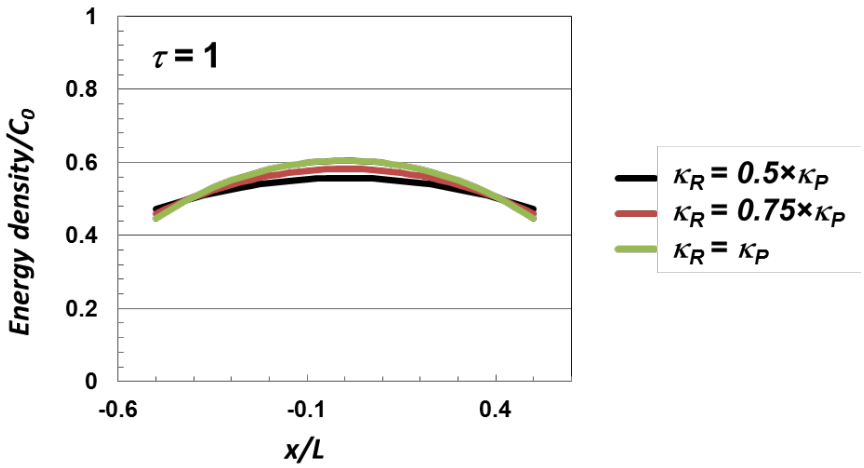


Fig. 2c: As Fig. 2a, but for a slab of Planck optical thickness 1.

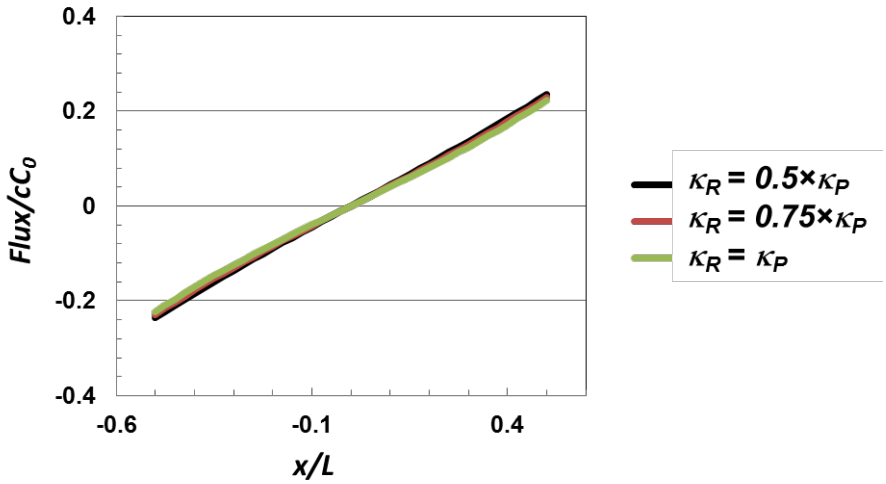


Fig. 2d: As Fig. 2c, but for spectral flux, plotted in units of $cC_0$.

## 4. Determining the Impact of the Rosseland-Averaged vs. Planck-Averaged Opacity

We will now analyze the impact of replacing the Rosseland-averaged opacity with the Planck-averaged opacity in a multigroup solution to the slab-source problem. We will set the

thickness of the slab to be 40 microns. The opacity, temperature, and ionic density are the same as those used to create Figure 1.

Figure 3 shows the ratio of the two-opacity to the one-opacity scale lengths $\lambda_{PR}/\lambda_P$ obtained using Eqs. (3.2) and (3.5), plotted as a function of photon energy. The opacities are group-averaged, which accounts for the step-function appearance. The variation in the scale length stays at around 10% until the final group where it rises to 20%. This is because the final group has a silicon spectral line, causing the Planck-averaged opacity to be significantly larger, thereby causing the scale length computed using solely the Planck-averaged opacity to be significantly smaller.

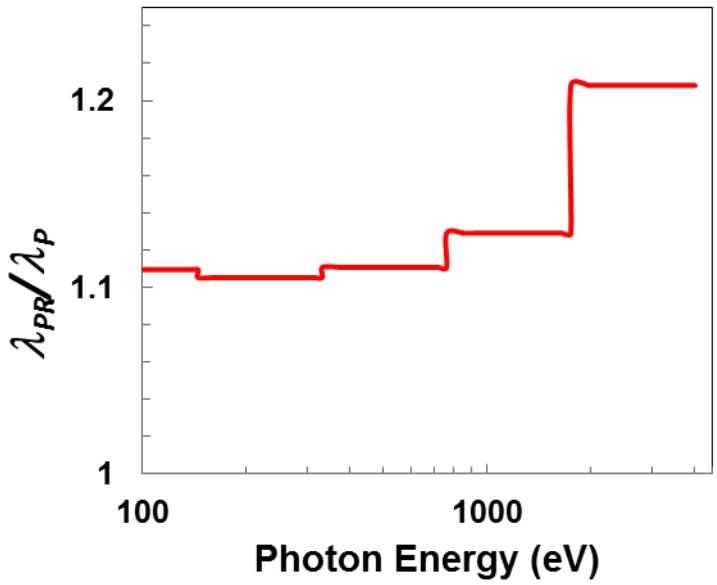


Figure 3: A graph of the ratios of the scale lengths $\lambda_{PR}/\lambda_P$ computed using a 1-opacity vs. a 2-opacity model.

We now evaluate Eqs. (3.1) for the radiation spectral flux for the same slab and the same conditions for each of the energy groups shown in Fig. 3, first with distinct $\kappa_P$ and $\kappa_R$, and then

substituting $\kappa_P$ for $\kappa_R$. The difference in the two flux spectra plotted in Figure 4(a) shows the impact of using the Planck-averaged opacity in both Eqs. (2.4), rather than both the Planck and Rosseland averages, where indicated.

The spectral fluxes, plotted in Fig. 4(a) in arbitrary units, do not appear as step functions, as they would if Eqs. (3.1) had been evaluated entirely in terms of group-averaged quantities, as has been described thus far. The actual calculation was performed using a frequency-dependent emissivity $\varepsilon(\nu)_k$ ,

$$\varepsilon(\nu)_k = 4\pi\kappa_{P,k}B_\nu(T), \tag{4.1}$$

where the frequency $\nu$ lies within the group boundaries $\nu_{k+1}$ and $\nu_k$. This is an attempt to restore some of the frequency dependence of the emissivity lost in the group-averaging process by using the Planck function itself, rather than its group average, as in Eq. (2.11). This does not recover all the spectral detail of the opacity within the frequency groups, particularly the strong spectral line seen in Fig. 1 in the highest energy group near 2000 eV.

The ratio of the one-opacity flux to the two-opacity flux plotted in Fig. 4(a) is plotted in Fig. 4(b). The sub-group frequency dependence of the emissivity, given by Eq. (4.1), cancels out of this flux ratio, restoring the step-function result that would have been obtained had Eq. (2.5) been used. It can be seen that the spectral flux computed by using solely the Planck-averaged opacity is greater by a small percentage for the smaller photon energy groups. However, for the higher energies, the flux computed using solely the Planck-averaged opacities is significantly, 15-25%, lower. This is due to the spectral lines of silicon appearing in this photon energy range

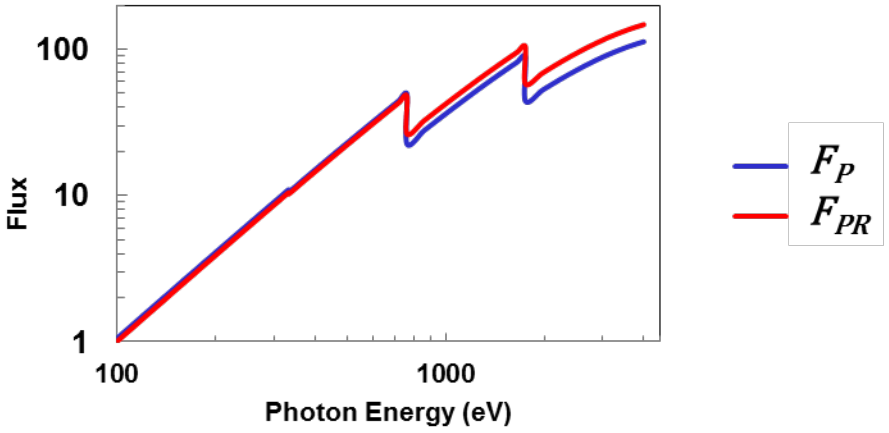


Figure 4a: Graphs of fluxes, expressed in arbitrary units, as functions of photon energy, comparing 1-opacity (blue curve) and 2-opacity (red curve) models.

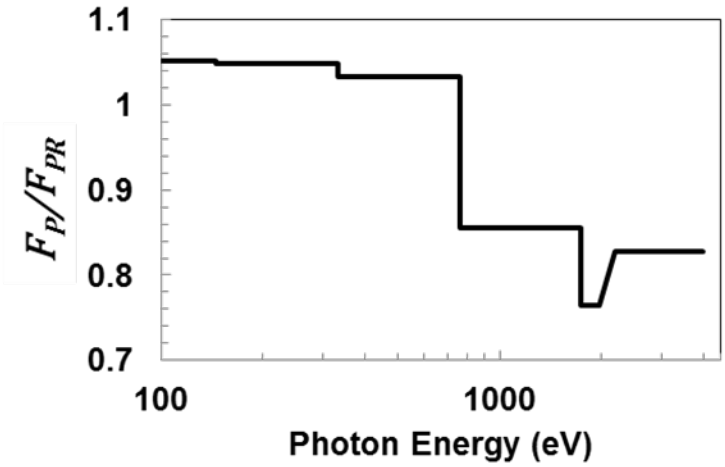


Figure 4b: Graph of the ratio of the fluxes computed by the one-opacity and two-opacity models as a function of photon energy.

lowering the Rosseland-averaged opacity, resulting in a longer scale length with less of the emitted photons being absorbed before they escape.

A 15-25% error is clearly too large to be ignored and calls into question the accuracy of one-opacity calculations in general, particularly if there is concern that an insufficient number of

photon energy groups are being used. Our preliminary results suggest that upgrading a one-opacity calculation to a two-opacity calculation may be an efficient complement to increasing the accuracy of calculations by increasing the number of energy groups. This conclusion is based only on our experience with the one example shown above. Before recommending that a simulation code be upgraded to include a two-opacity model, other examples will have to be studied, including realistic simulations of relevant experiments, as well as idealized configurations in addition to the slab model considered here.

## 5. Conclusions

In conclusion, we have demonstrated, by example, the possible benefit of upgrading from a one-opacity to a two-opacity model. Planck and interval-averaged opacities for Si were obtained by running the Prism detailed atomic model in the code *PROPACEOS*. An analytic solution was then derived for the radiation diffusion equation in a slab-source problem in which either the same or separate opacities were used for absorption and transport, and the calculated emitted spectral fluxes were compared. Even when the Planck and Rosseland averages differed, the differences in flux were minimal except for spectral intervals where the optical depth was approximately 1. There, it was shown that the values for flux can differ by ~10% - 20%. A broad range of conditions with a larger set of test cases will be necessary to establish the importance of changing from one-opacity to two-opacity modeling, but this work has laid some of the groundwork for how this is to be done, particularly the solution to the slab problem expressed in terms of both the Rosseland- and Planck-averaged opacities, which will allow a

broad range of cases to be considered. Thus far, it appears that upgrading to two-opacity modeling merits serious consideration.

## References


1. C. A. Haynam, P. J. Wegner, J. Auerbach, M.W. Bowers, S. N. Dixit, G. V. Erbert, G. M. Heestand, M. A. Henesian, M. R. Hermann, K. S. Jancaitis, K. R. Manes, C. D. Marshall, N. C. Mehta, J. Menapace, E. Moses, J. R. Murray, M. C. Nostrand, C. D. Orth, R. Patterson, R. A. Sacks, M. J. Shaw, M. Spaeth, S. B. Sutton, W. H. Williams, C. C. Widmayer, R. K. White, S. T. Yang, and B. M. Van Wonterghem, Appl. Opt. **46**, 3276-3303 (2007).

2. J. Nuckolls, L. Wood, A. Thiessen, and G. Zimmerman, Nature **239**, 139 (1972); Lois H. Gresh, Robert L. McCrory, and John M. Soures, *Inertial Confinement Fusion: An Introduction*, Laboratory for Laser Energetics: Rochester, NY, 2009.

3. V. N. Goncharov, "Cryogenic Deuterium and Deuterium-Tritium Direct-Drive Implosions on Omega," in *Laser-Plasma Interactions and Applications,* Scottish Graduate Series **68**, Springer International Publishing, P. McKenna, D. Neely, R. Bingham, D. A. Jaroszynski, eds., 2013.

4. T. R. Boehly, D. L. Brown, R. S. Craxton, R. L. Keck, J. P. Knauer, J. H. Kelly, T. J. Kessler, S. A. Kumpan, S. J. Loucks, S. A. Letzring, F. J. Marshall, R. L. McCrory, S. F. B. Morse, W. Seka, J. M. Soures, and C. P. Verdon, Opt. Commun. **133**, 495 (1997).

5. J. Delettrez, R. Epstein, M. C. Richardson, P. A. Jaanimagi, and B. L. Henke, Phys. Rev. **A 36**, 3926 (1987).

6. R. Epstein, *Equation of Transfer*, privately circulated report, Laboratory for Laser Energetics, Rochester, 2009.

7. S. Chandrasekhar, *Radiative Transfer*, Dover Publications, New York, 1960; J. I. Castor, *Radiation Hydrodynamics*, Cambridge University Press, 2004.

8. G. C. Pomraning, *The Equations of Radiation Hydrodynamics*, Pergamon Press, Oxford, 1973.

9. H. R. Griem, *Principles of Plasma Spectroscopy*, Cambridge University Press, Cambridge, England, 1997.

10. J. J. MacFarlane *et al.*, *PrismSPECT and SPECT3D Tools for Simulating X-ray, UV, and Visible Spectra for Laboratory and Astrophysical Plasmas*, American Physical Society, 34th Meeting of the Division of Atomic, Molecular and Optical Physics, May 2003; PrismSPECT, Prism Computational Sciences, Inc., http://www.prism-cs.com/

11. J. J. MacFarlane, I. E. Golovkin, P. R. Woodruff, J. Quant. Spectrosc. Radiat. Transfer **99**, 381-397 (2006).

## Acknowledgements

Working at the Laboratory for Laser Energetics was one of the most memorable and fulfilling experiences of my life. I would like to thank Dr. Craxton for running the high-school intern program and extending me the opportunity to work at the Laboratory for Laser Energetics. Dr. Reuben Epstein has my eternal gratitude for not only introducing me to the world of scientific research with an interesting project, but also taking me under his wing in every way. I would also like to thank my fellow interns for assisting me with various challenges along the way. Finally, I would like to express my appreciation to all of my teachers, friends, and family members for guiding me towards this path and supporting me in every endeavor.